Regular Contributed Papers

Acta Cryst. (1988). A44, 987-998

Propagating Local Positional Order in Tetrahedrally Bonded Systems

BY YASUSHI ISHII*

Lyman Laboratory of Physics, Harvard University, Cambridge, MA 02138, *USA*

(*Received* 16 *December* 1987; *accepted* 6 *April* 1988)

Abstract

Several possible aperiodic tetrahedrally bonded structures are investigated based on the concept of propagating local positional order. Local positional order (LPO) in a tetrahedrally bonded system is parametrized by the angle of relative rotation of tetrahedral coordinations of adjacent atoms, θ. By choosing θ appropriately we can have LPO which is incompatible with periodic translational order. Propagation of LPO is described here by rolling polytope $\{5, 3, 3\}$ and polytope 240. Defects of LPO in a system filled with atoms by a rolling polytope are discussed. As an alternative model, a three-dimensional Penrose tiling with tetrahedral decoration is investigated. It is shown that the proposed decoration necessarily introduces atoms with a broken bond.

1. Introduction

The structure of metallic glass is well simulated by the dense random packing (DRP) model (Finney, 1970). [For the relevance to metallic glasses, see Cargill (1975).] In the DRP model, four particles form a tetrahedral cluster to minimize the local energy density. When 20 tetrahedra meet at one vertex to form a 13-atom cluster, gaps appear between surface atoms because an edge of an icosahedron is about 5% longer than its center-to-vertex distance. This means that the local energy density cannot be minimized in a 13-atom cluster as much as in a four-atom tetrahedral cluster because a surface atom cannot sit in a site which minimizes pairwise energies simultaneously with its all neighbors. In this sense, there is structural frustration in DRP structure and icosahedral arrangements (Nelson, 1983*a*). However, if the clusters are small enough, icosahedral clusters have a significantly lower energy than 'crystalline' clusters such as clusters with a local atomic arrangement in face-centered cubic (f.c.c.) or hexagonal close-packed (h.c.p.) structures (Frank, 1952). Steinhardt, Nelson & Ronchetti (1983) have found in their molecular dynamics simulation that icosahedral bond orientational order can persist over distances of order at least three to four particle spacings in supercooled liquids.

Recently important progress has been made in describing local icosahedral order and its frustration. An icosahedral arrangement of points nicely fits on the surface of a four-dimensional sphere S^3 (Coxeter, 1983; Kléman & Sadoc, 1979). Because the frustration is eliminated by increasing the curvature of a space continuously, one expects that the frustration is parametrized by the curvature of a manifold which yields no frustration. Nelson (1983*a*) suggested that the local orientation of an icosahedron, $\mathbf{l}$, propagates so as to satisfy the condition of parallel transport

$$\delta_i l^j - \Gamma^j_{ki} l^k = 0, \qquad (1.1)$$

where Γ^j_{ki} is the connection coefficient for the curved manifold without frustration. When an icosahedron is parallel transported along a closed path, its orientation is rotated as $\Delta l^j = \oint \Gamma^j_{ki} l^k \, dx^i$, which, in general, does not vanish. To maintain the icosahedral order, this rotation should be one of the symmetry operations of an icosahedron. Therefore frustration induces defects of the icosahedral order. Sethna (1985) proposed a more general picture of parallel transport, in which the propagation of icosahedral order is described as the rolling of polytope $\{3, 3, 5\}$ (Coxeter, 1983; Kléman & Sadoc, 1979), in which 120 particles are placed on S^3 so that every particle has complete icosahedral coordination. Nelson & Widom (1984) developed this point of view more thoroughly. Sachdev & Nelson (1985) have calculated the density correlation function of a system with propagating icosahedral order based on Nelson & Widom's (1984) model and obtained a good agreement with experimental results for metallic glasses.

The propagating icosahedral positional order is realized in Frank-Kasper phases of transition-metal alloys. Frank & Kasper (1958, 1959) pointed out that structures of some transition-metal alloys can be understood as a packing of spheres and that an icosahedral atomic arrangement is prevalent in their structures. Nelson (1983*a*) has shown that the Frank-Kasper phases are regarded as ordered networks of defect lines of the icosahedral orientational order, *i.e.* disclinations. Widom (1987) has demonstrated that the $Mg_{32}(Al, Zn)_{49}$ structure is obtained by rolling

* Permanent address: The Institute for Solid State Physics, The University of Tokyo, Roppongi, Tokyo 106, Japan.

0108-7673/88/060987-12$03.00

polytope {3, 3, 5} and then a disclination is introduced in a natural way through the rolling polytope.*

The discovery of quasicrystals (Shechtman, Blech, Gratias & Cahn, 1984; Henley 1987), which are alloys exhibiting sharp diffraction patterns with icosahedral symmetry, has provided us with further insight into aperiodic structures. The long-range icosahedral orientational order can be achieved by making translational order *quasiperiodic* rather than *periodic* (Levine & Steinhardt, 1984). Here it is considered that the local positional order propagates in a coherent fashion through a long-range positional correlation in a higher-dimensional space. Although the relationship between quasicrystalline order and frustration in the icosahedral order is clearly complex, at least some of the quasicrystals can be viewed as ordered networks of disclination lines (Henley & Elser, 1986).

We have seen so far that the propagation of the local positional order (LPO) with a frustration tends to make a system aperiodic. In metallic systems, LPO is the icosahedral orientational order. In covalent systems, on the other hand, an atom has a directional bonding, which determines a different kind of LPO. In a diamond (zincblende) structure, a tetrahedral positional order is extended to infinite volume without frustration. However, it should be noticed that there is some restriction in a diamond structure. That is, the rotation of tetrahedra along their common axis is restricted to be 60°. Actually, by allowing this angle to take a different value, we get other crystalline structures such as a wurtzite one (Wells, 1977) and also non-crystalline ones (Polk, 1971; Connel & Temkin, 1974). Therefore we consider that the propagation of LPO plays an important role in structures of covalent substances as well. It is our purpose to investigate several possibilities of aperiodic covalent (tetrahedrally bonded) structures based on the concept of propagating local positional order (Mosseri, DiVicenzo, Sadoc & Brodsky, 1985).

To find LPO in a tetrahedrally bonded network, the orientation of tetrahedral bonds of adjoining atoms is an important parameter. The configuration of two atoms connected by a tetrahedral bond is parametrized by an angle of the relative rotation of tetrahedral coordinations, θ. The configuration corresponding to $\theta = 60°$ is called *staggered* and $\theta = 0°$ *eclipsed* (Wells, 1977). If all four tetrahedral bonds connected to a central atom are staggered, 12 atoms in a second coordination shell form a local atomic arrangement in f.c.c. structure. If one bond is eclipsed and the others are staggered, 12 atoms form an arrangement in h.c.p. structure (Fig. 1). Therefore the choice of θ determines LPO. It should also be noticed that, if we allow only eclipsed bonds, we have a planar configuration. Since the bond angle of a tetrahedral coordination, $\cos^{-1}(-1/3) \simeq 109{\cdot}4°$, is very close to the internal angle of a regular pentagon, 108°, the planar configuration leads to five-membered rings with only slight distortions; these rings are incompatible with a long-range translational order, however. Therefore the choice of θ also enables us to have LPO including a five-membered ring.

Quantum-mechanical calculations of chemical bonds give the energetic preference of an orientation of tetrahedral bonds of adjoining atoms (Pauling, 1960). However, it is interesting to note that the structural energy of a tetrahedrally bonded system is usually analyzed by using two- and three-body classical interatomic potentials, which are associated with bond-length and bond-angle variations, respectively (Keating, 1966; Biswas & Hamman, 1985). As the structural energy difference associated with θ is expressed in terms of a negligible four-body interatomic potential, it is expected that we are free from strong restrictions about θ in modeling LPO.

In § 2, we investigate the propagating LPO for $\theta = 0°$. As mentioned above, a planar five-membered ring is a basic unit when only an eclipsed bond is allowed. Then, as a fundamental cluster, we have a dodecahedral cage, which consists of 20 atoms and 12 five-membered rings. The propagation of LPO represented by a dodecahedral cage will be given by a rolling of polytope {5, 3, 3} which is dual to polytope {3, 3, 5}. Defects in this model will be discussed. In § 3 we study a different sort of icosahedral positional order with a covalent bonding by choosing $\theta \simeq 38°$. The propagation of this order is given by a rolling of polytope 240, which is decorated polytope {3, 3, 5} (Sadoc & Mosseri, 1982). Since polytope 240 has a lower symmetry than polytope {5, 3, 3}, defects which differ from the usual disclinations are expected. In Penrose tilings, tetravalent icosahedral orientational order propagates in a different way from a rolling polytope. In § 4 we try to make a quasicrystal with covalent bonding by arranging decorated tiles in a way to give Penrose tiling. It turns out that decoration

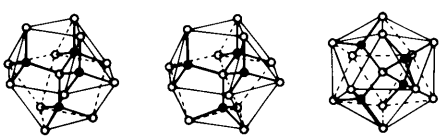

Fig. 1. Local atomic arrangements generated with tetrahedral atoms.

* In Laves phases and $Mg_{32}(Al, Zn)_{49}$ structures, all the icosahedral sites are accessible by a rolling polytope in the direction of a fivefold axis. Therefore the structure is described completely by the rolling polytope model. In the other Frank–Kasper phases, however, structures cannot be obtained only from a rolling polytope. For example, in the μ phase, we have a layer which is obtained by a rolling polytope but the stacking of layers is not determined by rolling.

of tiles necessarily generates decoration of vertices inconsistent with a covalent bonding.

2. Rolling polytope {5, 3, 3}

When only eclipsed bonds are allowed, a planar five-membered ring is a basic structural unit. Extending an eclipsed configuration further, we have a dodecahedral cage, which consists of 20 atoms with approximately tetrahedral coordination and 12 five-membered rings. A dodecahedral atomic arrangement is of course incompatible with translational order in a flat space but fits nicely on S^3. So a template of LPO in this case is provided by polytope {5, 3, 3} (Sadoc & Mosseri, 1982).

Polytope {3, 3, 5} can be triangulated into an assembly of 600 tetrahedra. Suppose that we place a point at the center of each tetrahedron and connect the points in tetrahedra sharing a face with each other. Then we have a new object which consists of 600 vertices with a tetrahedral bonding. This is polytope {5, 3, 3}. As is clear from the above construction, polytope {5, 3, 3} and polytope {3, 3, 5} are dual to each other and related in a similar way to the relation between Voronoi and Dirichlet constructions of networks (Collins, 1972). The symmetry of polytope {5, 3, 3} is the same as that of polytope {3, 3, 5}, which is $Y' \times Y'/Z_2$ where Y' is a lift of icosahedral point group Y into SU(2) and Z_2 is the two-element group (Nelson & Widom, 1984).

Propagation of LPO is given by rolling the polytope as follows: (1) Place polytope {5, 3, 3} so that S^3 has a contact with a flat physical space R^3 at the center of a dodecahedral cage. (2) Project the atomic arrangement near a tangential point onto a flat space R^3. (3) Roll polytope along a straight line, which is a trace of a geodesic line between centers of neighboring dodecahedral cages on S^3. (4) Repeat procedures (2) and (3) to fill a flat space with atoms. Because the centers of dodecahedral cages in polytope {5, 3, 3} are at the positions of vertices in polytope {3, 3, 5}, filling space with atoms by rolling polytope {5, 3, 3} is quite similar to that with polytope {3, 3, 5} demonstrated by Widom (1987).

To be more precise let us consider rolling a polytope in the direction of one of the fivefold axes, $\mathbf{e}_v$. Suppose that a north pole of the polytope touches R^3 at $\mathbf{r}$. By projecting an atomic arrangement around the north pole, we have a dodecahedral cage at $\mathbf{r}$. Then by rolling a distance $d_5 = R \times \pi/5$ where R is a radius of S^3, one of the centers of the dodecahedral cages neighboring the north pole of the polytope touches R^3 at the point $\mathbf{r} + d_5\mathbf{e}_v$. Projecting an atomic arrangement around the tangential point, we have another dodecahedral cage at $\mathbf{r} + d_5\mathbf{e}_v$, which is rotated by $\pi/5$ and shares a five-membered ring with that at $\mathbf{r}$. Since the rotation by $\pi/5$ is not a symmetry operation of a dodecahedron, another rolling by d_5 in the same direction is required to maintain the dodecahedral positional order. Then we have another dodecahedral cage at $\mathbf{r} + 2d_5\mathbf{e}_v$, which has the same orientation as that at $\mathbf{r}$ (more exactly, rotated by $2\pi/5$) (Fig. 2).

According to homotopy theory (Mermin, 1979), the algebra of defects of the dodecahedral order is given by $Y' \times Y'$ (Nelson & Widom, 1984). That is, the order parameter is transformed as a result of going along a loop encircling a defect as expressed in terms of a rotation of S^3 as

$$(l, r): \hat{u} = l\hat{u}r^{-1}, \tag{2.1}$$

where $l, r \in Y'$ (Appendix A). Since

$$(l, r): \hat{u} = (r, r): (r^{-1}l, \hat{1}): \hat{u}, \tag{2.2}$$

a defect is generally a combination of a net rotation and a screw transformation. If we confine our discussion to a rotational defect, *i.e.* disclination, the algebra of defects is simply given by (Nelson, 1983*a*)

$$\pi_1[\mathrm{SO}(3)/Y] = Y' \tag{2.3}$$

Then a disclination is characterized by a rotation angle and a rotation axis of a dodecahedral symmetry operation (see Appendix B). In fact, as a result of rolling along a rhombic plaquette (edge length $= 2d_5$) spanned by two of the vertex vectors of an icosahedron, a dodecahedral cage rotates by $2\pi/5$ around one of the fivefold axes. This defect is called a $-72°$ disclination, the minus sign indicating that the defect is obtained by adding a wedge of material. As is clear from Fig. 3, the structure of a core of this defect is a planar six-membered ring through which a disclination line threads. We can imagine a disclination of a topological charge $+72°$ which threads through four-membered rings. However, if we try to make a ring only with eclipsed configurations by keeping bond

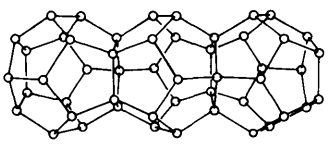

Fig. 2. Chain of dodecahedral cages obtained by successively rolling polytope {5, 3, 3} along a fivefold axis.

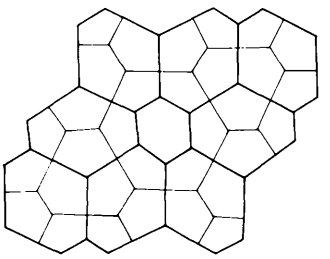

Fig. 3. Core structure of $-72°$ disclination obtained by rolling polytope {5, 3, 3} along a rhombic plaquette spanned by two of the vertex vectors of an icosahedron.

angles strictly $\cos^{-1}(-1/3)$, a gap opens for a five-membered ring with a deficit angle $\simeq 7{\cdot}356°$. Therefore there is a tendency that six-membered rings are more prevalent than four-membered ones.

The rolling polytope {5, 3, 3} model gives porous structures because a dodecahedral cage has a large hole inside. Note that the diameter of a dodecahedron is $3^{1/2}\tau \simeq 2{\cdot}80$ for a vertex-vertex distance or $\tau^3/(\tau^2+1)^{1/2} \simeq 2{\cdot}23$ for a face-face distance where the edge length of a dodecahedron is taken to be unity. (τ is the golden mean.) In fact, the propagating dodecahedral positional order described by the rolling polytope {5, 3, 3} is realized in some clathrate compounds, M_xT_y where M and T are an interstitial molecule and a tetrahedral unit, respectively. Frank & Kasper (1959) pointed out in their pioneering work that structures of some gas hydrates ($T = H_2O$) are dual to Frank-Kasper alloys. There water molecules form a dodecahedral cage or cages dual to $Z14$, $Z15$ and $Z16$ configurations in a defect core. Furthermore dual structures to Laves phase (M_xT_{136}) and $A15$ (M_xT_{46}) have been observed in some silica compounds ($T = SiO_2$) (Shenker *et al.*, 1981) and alkali-metal silicides (T = Si) (Cros, Pouchard & Hagenmuller, 1970). Here it should be noted that an interstitial molecule plays a crucial role in stabilizing these structures. Recently Mackay (1985) proposed a decoration of Penrose tiles based on a dodecahedral cage. To stabilize this hypothetical quasicrystal, an interstitial molecule will be very important.

3. Rolling polytope 240

The diamond structure is made only from staggered ($\theta = 60°$) bonds whereas a system with propagating dodecahedral positional order is made only from eclipsed ($\theta = 0°$) bonds. The wurtzite structure is a mixture of staggered and eclipsed bonds with a bulk ratio 3:1. In this section we explore the possibility of LPO with an intermediate value of θ.

Let us consider a configuration of 17 atoms, in which one atom is connected with four atoms, each of which has three other neighboring atoms, by tetrahedral bonds characterized by θ. Then the coordinates of the 12 atoms in the outermost coordination shell are given by

$$\begin{aligned}\mathbf{r} &= (4/3\sqrt{3})(+[1+\cos\theta], +[1-\cos(\theta+\pi/3)], \\ &\qquad +[1-\cos(\theta-\pi/3)]), \\ &= (4/3\sqrt{3})(-[1+\cos\theta], -[1-\cos(\theta+\pi/3)], \\ &\qquad +[1-\cos(\theta-\pi/3)]), \\ &= (4/3\sqrt{3})(-[1+\cos\theta], +[1-\cos(\theta+\pi/3)], \\ &\qquad -[1-\cos(\theta-\pi/3)]), \\ &= (4/3\sqrt{3})(+[1+\cos\theta], -[1-\cos(\theta+\pi/3)], \\ &\qquad -[1-\cos(\theta-\pi/3)]), \end{aligned} \tag{3.1}$$

and their even (cyclic) permutations where the length of a tetrahedral bond is taken to be unity and the (1, 1, 1), (1, −1, −1) (−1, 1, −1) and (−1, −1, 1) directions are chosen to be threefold axes of tetrahedral coordination. We can assume here that θ varies in the range $-\pi/3 < \theta \leq \pi/3$ because the location of 12 atoms is invariant under a change of $\theta \to \theta + 2\pi/3$. Furthermore a change of sign of θ gives the coordinates obtained by odd permutation of the original one. Therefore a change of sign of θ is associated with *chirality* of LPO.

The interatomic distance between atoms in the outermost shell is shown in Fig. 4 as a function of θ. Note that we have at about $\theta = 38°$ a configuration very similar to that in an icosahedron; five nearest-neighbor, five second-neighbor and one third-neighbor atoms at distances of $2a\sin(\theta/2) \simeq 2a \times 0{\cdot}525$, $2a\cos(\theta/2) \simeq 2a \times 0{\cdot}850$ and $2a$, respectively, where $\cos\theta = 1/\sqrt{5}$ and the center-to-vertex distance of an icosahedron $a \simeq 1{\cdot}71$ in the present case. Actually it is possible to decorate a 13-atom icosahedral configuration with four atoms connected to a centered atom by approximate tetrahedral bonds. In this configuration, we find θ to be $\cos^{-1}(5/8)^{1/2} \simeq 37{\cdot}76°$.

A template of this local atomic arrangement is provided by polytope 240 (Sadoc & Mosseri, 1982) which is obtained from polytope {3, 3, 5} in a similar way to the construction of the diamond structure from a f.c.c. lattice; the diamond structure consists of two f.c.c. sublattices, one of which is obtained by translation of the other. Coordinates of a point in the B sublattice are given by

$$\hat{u}_B = \hat{u}_A \exp(i\hat{\sigma}_x\pi/4) \tag{3.2}$$

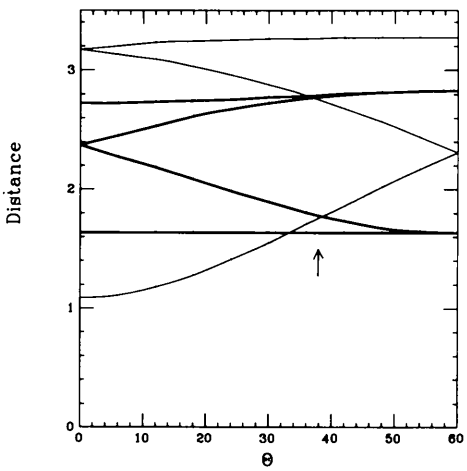

Fig. 4. Interatomic distances in a second coordination shell of a 17-atom cluster made from tetrahedral bonds characterized by θ. Thick curves should be regarded as indicating that two atoms are located at the same distance. The arrow indicates a position giving an approximate icosahedral configuration.

for polytope 240 with right chirality and

$$\hat{u}_B = \exp(i\hat{\sigma}_x\pi/4)\hat{u}_A \tag{3.3}$$

for that with left chirality, where $\hat{u}_A$ is a quaternion representation of the coordinates of the vertex in polytope $\{3, 3, 5\}$ (Mosseri *et al.*, 1985). Here right and left chirality correspond to positive and negative values of θ, respectively.

The symmetry group of polytope 240 with right chirality is expressed as $Y' \times T'/Z_2$ (Mosseri *et al.*, 1985) if two sublattices are distinguishable.* Here T' is a lift of the tetrahedral point group into SU(2) (Appendix *B*). This can be shown as follows. Consider a transformation of a point in polytope 240, $\hat{u}$, given by $(l, r):\hat{u}$ where $l \in Y'$ and $r \in T'$. Since a set of vertices of polytope $\{3, 3, 5\}$ is isomorphic to Y', we have a relation

$$\hat{u} \in Y' + Y' \exp(i\hat{\sigma}_x\pi/4). \tag{3.4}$$

If $\hat{u}$ is an element of Y', (l, r): $\hat{u}$ is also an element of Y' because T' is a subgroup of Y'. If $\hat{u}$ is an element of $Y' \exp(i\hat{\sigma}_x\pi/4)$, then

$$(l, r)\text{: } \hat{u} \in Y' \exp(i\hat{\sigma}_x\pi/4)T'. \tag{3.5}$$

Since

$$\exp(i\hat{\sigma}_x\pi/4)T' = T' \exp(i\hat{\sigma}_x\pi/4), \tag{3.6}$$

$(l, r):\hat{u}$ is an element of $Y' \exp(i\hat{\sigma}_x\pi/4)$. Therefore $(l, r):\hat{u}$ ($l \in Y'$ and $r \in T'$) is a symmetry operation of polytope 240 with right chirality. The symmetry group of polytope 240 with left chirality is given by $T' \times Y'/Z_2$.

By rolling polytope 240, we try to fill a space with tetrahedrally bonded atoms in an icosahedral atomic arrangement. To maintain the icosahedral order, it is required to roll the polytope along a geodesic line joining two vertices in one sublattice, which is polytope $\{3, 3, 5\}$. A rotation of S^3 induced by the rolling along a geodesic line joining vertices on polytope $\{3, 3, 5\}$ is given by $(l, l^{-1}):\hat{u}$ where $l^2 \in Y'$. Since

$$(l, l^{-1}):\hat{u} = (l^{-1}, l^{-1}):(l^2, \hat{1}):\hat{u}, \tag{3.7}$$

and

$$(l^2, \hat{1}):\hat{u} \in Y' + Y' \exp(i\hat{\sigma}_x\pi/4), \tag{3.8}$$

a rotation of a local atomic arrangement projected onto a real space R^3 induced by rolling polytope 240 is described as $(l, l):\hat{u}$ where $l^2 \in Y'$. By successive rolling in the same direction, a local atomic arrangement projected onto a real space R^3 rotates as $(l^2, l^2):\hat{u}$. This rotation is a symmetry operation of polytope $\{3, 3, 5\}$ but not in general that of polytope 240. In other words, the icosahedral orientation order is maintained by the successive rolling in the same direction but the orientational order of tetrahedral decoration cannot be conserved generally.

The algebra of defects of the local positional order described by a template of polytope 240 is given by $Y' \times T'$. Hereafter we consider polytope 240 with right chirality. In this case we should regard $l \in Y'$ and $r \in T'$ in (2.2). Therefore the algebra of a rotational defect is given by

$$\pi_1[\mathrm{SO}(3)/T] = T', \tag{3.9}$$

whereas a screw defect is classified by Y'. Fundamental rotational defects in this case are $\pm 2\pi/3$ disclinations, which are characterized by a $2\pi/3$ rotation of the icosahedral atomic arrangement with tetrahedral decoration as a result of moving along a loop encircling a disclination line. Since $2\pi/3$ rotation of an icosahedron is generated by a combination of $2\pi/5$ rotations, $\pm 2\pi/3$ disclinations can be regarded as consisting of several defects associated with $2\pi/5$ rotations of an icosahedral framework as well as a defect of tetrahedral decoration.

In order to understand typical core structures of a defect of the orientational order with additional decoration, let us consider a two-dimensional system, which is easy to visualize. A two-dimensional (2D) analog to the icosahedral order in a three-dimensional (3D) flat space is provided by the hexagonal orientational order in a 2D negatively curved space (Nelson, 1983*a*; Rubinstein & Nelson, 1983). In the 3D case, four of 20 tetrahedra meeting at one vertex are decorated with a tetrahedrally bonded atom. In the 2D case, on the other hand, three of six triangles meeting at one vertex are decorated with trigonally bonded atoms as shown in Fig. 5.

Rotational defects of the hexagonal order are classified as

$$\pi_1[\mathrm{SO}(2)/C_6] = \{\mathcal{T}_{n\pi/3}\text{: } n = \text{integer}\}, \tag{3.10}$$

whereas those of the decorated hexagonal order are classified as

$$\pi_1[\mathrm{SO}(2)/C_3] = \{\mathcal{T}_{2n\pi/3}\text{: } n = \text{integer}\}, \tag{3.11}$$

where $\mathcal{T}_a$ is a generator of a one-dimensional translation by a (Mermin, 1979). Fundamental rotational

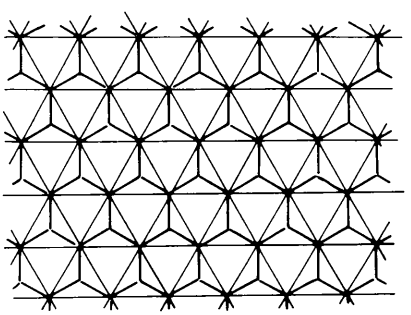

Fig. 5. Two-dimensional analog to the icosahedral order with tetrahedral decoration in three dimensions.

* If two sublattices are indistinguishable, the symmetry group is $Y' \times O'/Z_2$ where a lift of the octahedral point group into SU(2), O', is given by $O' = T' + T' \exp(i\hat{\sigma}_x\pi/4)$ (Mosseri *et al.*, 1985).

defects in a hexagonal ordered state are thus ±60° disclinations, which are characterized by a $\pi/3$ rotation of a hexagonal atomic arrangement as a result of moving along a loop encircling a defect. Since a $\pi/3$ rotation is not a symmetry operation of a trigonal decoration, a bond orientational order described by a decorated template should vanish somewhere along a loop encircling a ±60° disclination. As shown in Fig. 6, decoration around a −60° disclination results in a line of defects on which the bond orientational order vanishes, that is, a trigonal atomic arrangement fails. The core of this line defect consists of atoms with a broken (dangling) bond.

Broken bonds cost much energy in a covalent system where a chemical bond plays a primary role in structural energy. Then it is more plausible that a string of atoms with broken bonds is rearranged into a string of abnormal rings, which are rings other than hexagonal six-membered rings, as shown in Fig. 6. Note that the hexagonal bond orientational order vanishes along the string by this bond rearrangement. In a system in which the hexagonal order is promoted by a stronger interaction, on the other hand, the rearrangement disturbing the hexagonal order is less plausible. A physical example of this case will be provided by non-spherical molecules adsorbed on graphite, where ordering of molecular orientation takes place at lower temperatures (Zhang, Kim & Chan 1985). A string of defects of the trigonal decoration terminates at a disclination. Since the energy cost due to the defects is proportional to the length of a string, it is energetically favored that a string is stretched tightly between ±60° disclinations. Interaction between disclinations with topological charges of opposite signs is inherently attractive (Nelson & Halperin, 1979; Nelson, 1983*b*). Then strings of defects of the trigonal decoration are expected to cause additional attractive interaction between a pair of disclinations.

The bond orientational order is maintained along a loop encircling a pair of disclinations connected by a string of defects, which are abnormal rings, because a class multiplication of a homotopy group $\pi_1[\mathrm{SO}(2)/C_6]$ is given by

$$\begin{aligned} \{\mathcal{T}_{+\pi/3}\}\times\{\mathcal{T}_{-\pi/3}\}&=\{\mathcal{T}_0\},\\ \{\mathcal{T}_{-\pi/3}\}\times\{\mathcal{T}_{-\pi/3}\}&=\{\mathcal{T}_{-2\pi/3}\}, \end{aligned} \tag{3.12}$$

where $\{\mathcal{T}_0\}$ and $\{\mathcal{T}_{-2\pi/3}\}$ are elements of $\pi_1[\mathrm{SO}(2)/C_3]$. A pair of disclinations with opposite signs of topological charges is regarded as a dislocation (Nelson & Halperin, 1979; Nelson, 1983*b*). Therefore one of the fundamental defects of the hexagonal order with trigonal decoration is a dislocation, which is necessarily associated with a string of abnormal rings. In a negatively curved space, however, since −60° disclinations are more prevalent than +60° ones, they do not compensate each other completely. Then we have a pair of disclinations with negative topological charges as another defect (see Fig. 7).

For the icosahedral orientational order in 3D, since successive rolling polytopes along $2d_5\times\mathbf{e}_v^{(1)}$, $4d_5\times\mathbf{e}_v^{(2)}$, $2d_5\times(-\mathbf{e}_v^{(1)})$ and $4d_5\times(-\mathbf{e}_v^{(2)})$, where $\mathbf{e}_v^{(1)}=(\tau,1,0)/(\tau^2+1)^{1/2}$ and $\mathbf{e}_v^{(2)}=(1,0,\tau)/(\tau^2+1)^{1/2}$ are unit vectors in the direction of fivefold axes of an icosahedron, yield a rotation of the icosahedral arrangement by $2\pi/3$ around a $(1,1,-1)$ axis, this loop encircles a disclination associated with $2\pi/3$ rotation of the icosahedral arrangement with tetrahedral decoration. Considering that a rhombic plaquette spanned by $2d_5\times\mathbf{e}_v^{(1)}$ and $2d_5\times\mathbf{e}_v^{(2)}$ encircles a −72° disclination, we can regard this $2\pi/3$ rotational defect

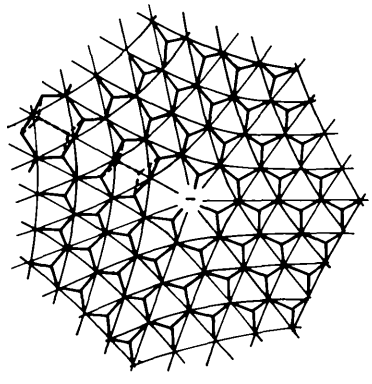

Fig. 6. Isolated −60° disclination decorated with trigonal atoms.

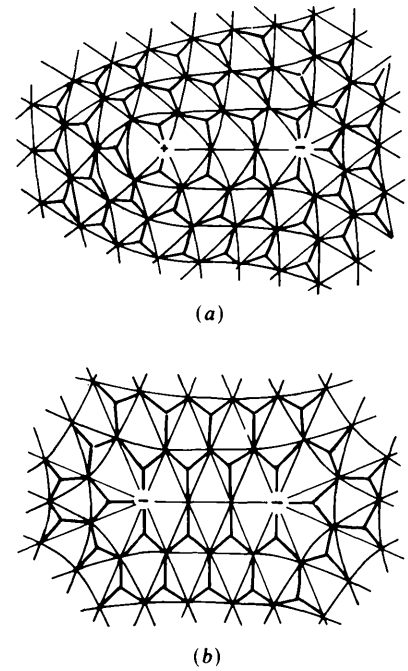

Fig. 7. Decoration of pairs of fundamental rotational defects of the hexagonal order with trigonal atoms. (*a*) (+, −) pair and (*b*) (−, −) pair.

as consisting of a combination of two $-72°$ disclinations. Note that the center of the loop has an icosahedral coordination but tetrahedral decoration of icosahedrally coordinated atoms is not consistent with that of the center. Then the center of the loop should be occupied by an atom with a broken bond. This is analogous to a pair of $-60°$ disclinations expected in a negatively curved 2D space.

We have another complicated aspect in 3D, however. According to homotopy theory (Mermin, 1979), it is not the individual element but the class structure that determines how defects combine. Since a homotopy group $\pi_1[SO(3)/Y]$ is non-Abelian, combination of defects is given in terms of quite non-trivial class multiplication (Nelson, 1983*a*). Actually successive rolling of a polytope along $4d_5 \times \mathbf{e}_v^{(2)}$, $2d_5 \times (-\mathbf{e}_v^{(1)})$, $4d_5 \times (-\mathbf{e}_v^{(2)})$ and $2d_5 \times \mathbf{e}_v^{(1)}$ yields a rotation by $2\pi/3$ around the $(0, \tau, 1/\tau)$ axis, which is not a symmetry operation of polytope 240. A $2\pi/3$ rotation which is a symmetry operation of polytope 240 is obtained only when we roll polytopes successively along paths shown in Fig. 8(*a*). Therefore LPO described by polytope 240 propagates successfully along the path shown in Fig. 8(*b*). There LPO at a point 1 propagates along a path II passing a point 2. Then LPO at a point 2 propagates along a path $-$III passing a point 3, which is another starting point of rolling. Note that LPO does not propagate successfully along the path shown in Fig. 8(*c*) because LPO propagating from a point 2 to a point 3 along a path I is related to that propagated along a path I′ by a $2\pi/3$ rotation around $(-1/\tau, -\tau, 0)$, which is not a symmetry operation of polytope 240. Although we have not succeeded in obtaining bulk structures explicitly, filling a space with tetrahedrally bonded atoms by rolling polytope 240 seems fairly difficult in the sense that reasonable paths of rolling are very restricted.

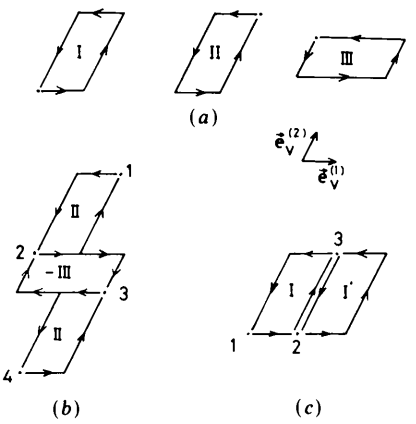

Fig. 8. (*a*) Paths along which the icosahedral order with tetrahedral decoration is maintained through rolling. (*b*) Possible way of propagation of the icosahedral order with tetrahedral decoration. (*c*) Path along which the icosahedral order with tetrahedral decoration does not propagate without frustration.

4. Decoration of Penrose tiling

In three-dimensional (3D) Penrose tiling, a space is filled with two kinds of rhombohedra, a prolate rhombohedron (PR) and an oblate one (OR), spanned by a triad of vertex vectors of an icosahedron. Therefore there is a long-range correlation of the icosahedral orientational order in 3D Penrose tiling. When 3D Penrose tiling is generated by means of a projection of a six-dimensional (6D) hypercubic lattice onto a 3D real space, a long-range correlation of the icosahedral orientational order is incorporated by requiring that six lattice vectors of the 6D hypercubic lattice are projected to give six vertex vectors of an icosahedron in a 3D real space. In this sense, the icosahedral orientational order propagates in a coherent way through a long-range positional correlation in a higher-dimensional space. In this section, we try to construct an aperiodic covalent system by decorating Penrose rhombohedral tiles with tetrahedrally bonded atoms. This provides us with an alternative model of the propagating LPO with tetrahedral bonding.

Our approach is similar to Elser & Henley's (1985; Henley & Elser, 1986) method for deriving realistic structures of quasicrystalline alloys. Elser & Henley (1985) proposed a projection scheme generating a rational approximation of 3D Penrose tiling, that is, a large unit-cell structure with Penrose rhombohedral tiles (Appendix *C*). They pointed out that the crystal structures of some alloys which have a similar chemical composition to that of quasicrystalline phases can be interpreted as a periodic Penrose lattice with an appropriate decoration and proposed possible quasicrystalline structures based on the decoration found in crystalline alloys. Although Penrose rhombohedral tiles are not necessarily fundamental structural units which reflect the chemical character of compositional elements, Elser & Henley's method is one reasonable way to analyze realistic structures of quasicrystallites.

Diamond (zincblende) and wurtzite structures are interpreted as packing of decorated rhombohedral tiles. By Dirichlet construction for f.c.c. and h.c.p. structures, a space is divided into an assembly of tetrahedra and octahedra in a 2:1 ratio. Since an octahedron capped with two tetrahedra makes a prolate rhombohedron, only slightly distorted with respect to a Penrose PR, we can regard f.c.c. and h.c.p. structures as packing of PR's. Here, the difference between f.c.c. and h.c.p. structures is that of stacking of rhombohedra. The diamond and wurtzite structures, which are derived from f.c.c. and h.c.p. lattices, respectively, are obtained by decorating the PR with a tetrahedrally bonded atom, as shown in Fig. 9.

It is known that tetrahedrally bonded Si has another cubic structure than diamond and wurtzite types under high pressure (Kasper & Richards, 1964). In

this high-pressure phase, which is usually referred to as BC-8 or Si III, a tetrahedrally bonded network is divided into two sublattices, one of which is obtained by translation of the other, as in the diamond and wurtzite structures. The sublattice structure in this case can be regarded as a packing of two kinds of rhombohedra, PR and OR, with a bulk ratio 1:1 where atoms occupy vertices of both rhombohedra. Remarkably, this packing of rhombohedra is topologically the same as one of the rational approximations of a 3D Penrose lattice, which is called 1/0 periodic structure (Elser & Henley, 1985). If we regard the BC-8 structure as a packing of decorated Penrose tiles, the PR and OR should be decorated as shown in Fig. 10.

Internal solid angles associated with each vertex of Penrose rhombohedral tiles are $\pi/5$, $3\pi/5$, $7\pi/5$, and $\pi/5$ for a vertex on a threefold axis of a PR (denoted as P_1), a vertex not on a threefold axis of a PR (P_3), a vertex on a threefold axis of an OR (O_7) and a vertex not on a threefold axis of an OR (O_1), respectively. Then a vertex in a Penrose lattice is classified in terms of the numbers of P_1, P_3, O_7 and O_1 tips meeting at the vertex (Henley, 1986). In a 1/0 periodic Penrose lattice, all eight vertices in a cubic unit cell are labeled as $(p_1, p_3, o_1, o_7) = (1, 3, 1, 3)$ where p_1 is the number of P_1 tips meeting at the vertex and so on. According to the decoration scheme in Fig. 10, all of P_1 and P_3 are decorated in such a way as to be connected by one bond while all of O_1 and O_7 are not decorated with any bond. Then eight vertices in a unit cell of 1/0 periodic structure are decorated with four bonds.

In a 1/1 periodic Penrose lattice, there are 32 vertices in a cubic unit cell, which are labeled as in Table 1. If we adopt the decoration scheme in Fig. 10 straightforwardly, a vertex labeled as (0, 2, 0, 2) is decorated by only two bonds, which is inconsistent with tetrahedral bonding. However, Elser & Henley (1985) proposed to eliminate vertices labeled as

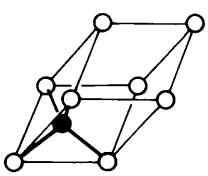

Fig. 9. Decoration of PR in diamond and wurtzite structures.

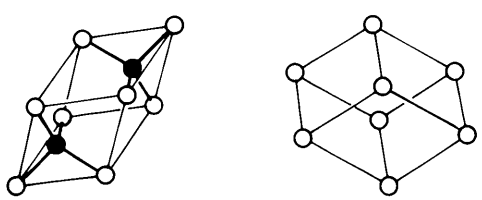

Fig. 10. Decoration of PR and OR in BC-8 structure.

Table 1. *Vertices in* 1/1 *periodic Penrose lattice*

Label	Number of vertices
$(0, 2, 0, 2)_0^*$	6
$(0, 4, 1, 1)_1^*$	6
$(1, 3, 3, 1)_1^*$	6
(0, 6, 2, 0)	6
(1, 5, 4, 0)	6
(14, 0, 6, 0)	2

* The subscript is the number of second neighbors along a chain of threefold body diagonals of OR.

(0, 2, 0, 2) by modifying a shadow space (Henley, 1986) and to take, as an additional structural unit, a rhombic dodecahedron (RD), which is made out of two PR's and two OR's. The internal solid angle of each vertex of RD is $2\pi/5$, $3\pi/5$, $4\pi/5$ and $7\pi/5$ as shown in Fig. 11. By eliminating vertices (0, 2, 0, 2) from the 1/1 structure, we have 26 vertices in a unit cell, which are classified as two vertices labeled as $(p_1, p_3, o_1, o_7, r_2, r_3, r_4, r_7) = (8, 0, 0, 0, 6, 0, 0, 0)$ and 24 vertices as (0, 2, 0, 0, 0, 1, 1, 1). In order to make all 26 vertices connected by four bonds, we require the following rules: (1) For a PR, half the P_1 and P_3 tips should be decorated with one bond. (2) For a RD, R_3, R_4 and R_7 tips should be decorated with one bond whereas R_2 tips should not be decorated. We find that decoration satisfying the above rules is given as shown in Fig. 12.

If the symmetry of a decorated tile is the same as that of the original one, the decoration of a whole system can be done quite automatically. If the symmetry of a tile is lowered by decoration (asymmetric decoration), however, a way of lowering symmetry should be determined for each tile by checking the

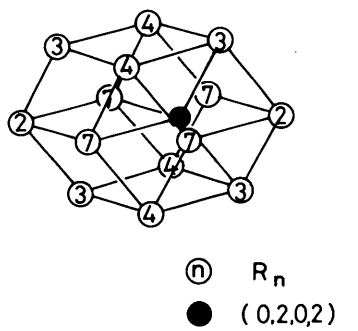

Fig. 11. Configuration around (0, 2, 0, 2) vertex and a RD tile.

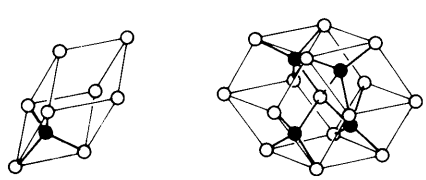

Fig. 12. Proposed decoration of PR and RD for 1/1 periodic Penrose lattice.

local environment. To be more precise, let us examine decoration of a PR and a RD in Fig. 12. There a PR loses an inversion symmetry in a decorated version whereas a mirror symmetry for a plane involving a twofold axis is not conserved in a decorated RD. Let us color rhombic faces which are decorated so that three vertices are connected with a single tetrahedral atom inside (Fig. 13). Then an additional restriction of decoration can be stated as follows: a colored face of one tile should be pasted on an uncolored face of the other. If a colored face is pasted on a colored one, we have a four-membered ring, which costs much structural energy. Actually, a 1/1 periodic Penrose structure can be decorated to satisfy the coloring-and-matching rule. In the resulting structure, all the vertices are connected by distorted tetrahedral bonds and there is no broken bond. By moving atoms appropriately without changing topology, we find that this structure is equivalent to the diamond structure.

Local atomic arrangements generated by the rolling polytope model minimize approximately the structural energy described by two- and three-body interactions because a template has correct tetrahedral coordination. Local atomic arrangements in a decorated periodic Penrose structure, on the other hand, cost a great deal of three-body interaction energy, which is associated with a bond-angle variation. To see this, let us parametrize the structural energy in terms of two- and three-body interatomic potentials as

$$E_{st}=\sum_i [\varepsilon_s(i)+\varepsilon_b(i)], \tag{4.1}$$

where $\varepsilon_s(i)$ and $\varepsilon_b(i)$ are the bond-stretching and bond-bending energies associated with the ith atom. Within the Keating (1966) model these energies are given by

$$\varepsilon_s(i)=\tfrac{1}{2}k_s\sum_j\left[\left(\frac{\mathbf{R}_j-\mathbf{R}_i}{a}\right)^2-1\right]^2,$$
$$\varepsilon_b(i)=\tfrac{1}{2}k_b\sum_{j>l}\left[\left(\frac{\mathbf{R}_j-\mathbf{R}_i}{a}\right)\left(\frac{\mathbf{R}_l-\mathbf{R}_i}{a}\right)+\tfrac{1}{3}\right]^2, \tag{4.2}$$

where $\mathbf{R}_i$ is the positional vector of the ith atom and summation is taken over tetrahedrally coordinated sites of the ith atom. Force constants k_s and k_b are taken as 12·4 and 7·08 eV, respectively, for Si and an equilibrium bond length a is taken to be $\sqrt{6}/4$, which is the center-to-vertex distance of a tetrahedron with a unit edge length. In Table 2 the stretching and bond-bending energies for inequivalent atoms in a unit cell in decorated 1/0 and 1/1 structures are shown. It is remarkable that there is atomic-scale inhomogeneity. We can relax a decorated structure to minimize the structural energy. Here it is assumed that the topology of the lattice is not changed, that is, rearrangements of bonds are not allowed in a relaxation process. After relaxation, the atomic-scale inhomogeneity is removed completely. The resulting systems are exactly BC-8 and diamond lattices for 1/0 and 1/1 periodic Penrose structures, respectively!

Table 2. *Structural energies of a decorated periodic Penrose lattice*

Lattice	Vertex*	Unrelaxed ε_s (eV)	Unrelaxed ε_b (eV)	Relaxed ε_s (eV)	Relaxed ε_b (eV)
1/0	*A*	0·08	1·85	0·05	0·50
	B	0·08	0·11	0·05	0·50
1/1	*A*(8, 0, 0, 0, 6, 0, 0, 0)	0·08	0·01	0·05	0·01
	A(0, 2, 0, 0, 0, 1, 1, 1)	0·08	1·55	0·05	0·01
	A in RD	0·08	4·50	0·05	0·01
	B in PR	0·08	0·11	0·05	0·01
	B in RD	0·08	2·60	0·05	0·01

* Vertices of Penrose tiles are designated as *A* while those added by decoration (black atoms in Figs. 7, 10 and 12) are designated as *B*.

We have obtained decoration of the structural units of Penrose tiling. Here it should be determined depending on the local environment, probably by using the coloring-and-matching rule explained above, whether a PR should be decorated with one tetrahedral atom or with two atoms. Actually, when we try to decorate higher-order periodic Penrose lattices, the coloring-and-matching rule in the case of asymmetric decoration makes it very difficult to find reasonable decorated structures. However, we can show that atoms with broken bonds are necessarily introduced in a decorated Penrose lattice. For example, a unit cell of 2/1 periodic structure consists of 84 PR's and 52 OR's in the original tiling and 49 PR's, 16 OR's and 18 RD's after eliminating (0, 2, 0, 2) vertices. Labels of vertices in both cases are shown in Table 3. Apparently decoration of vertices labeled as (0, 2, 0, 1, 0, 0, 0, 1), (0, 0, 1, 0, 0, 5, 1, 0), and (1, 0, 1, 0, 0, 2, 3, 0) are inconsistent with tetrahedral bonding because they are connected by three, six and five (at least) bonds, respectively, according to the decoration scheme derived above. This means that atoms with broken bonds are necessarily introduced in higher-order periodic Penrose lattices with tetrahedral decoration.

Recently Olami & Alexander (1987) have proposed a tetrahedrally coordinated quasicrystalline structure, which is obtained by projection of a 6D hypercubic lattice with non-symmorphic tetrahedral decoration onto a 3D real space. Since all the tetrahedrally coordinating sites in a 6D space are not always accepted to be projected onto a 3D space, the resulting structure inevitably involves many dangling bonds. Although the relationship between the present decoration of

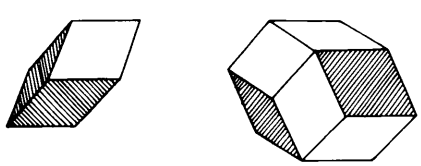

Fig. 13. Coloring of PR and RD decorated as in Fig. 12.

Table 3. *Vertices in 2/1 periodic Penrose lattice*

(p_1, p_3, o_1, o_7)	$(p_1, p_3, o_1, o_7, r_2, r_3, r_4, r_7)$	Number of vertices
$(0,2,0,2)_0$	Eliminated	6
$(0,2,0,2)_1$	Eliminated	12
$(0,2,0,2)_2$	(0, 2, 0, 0, 0, 0, 0, 2)	6
$(0,4,1,1)_0$	(0, 2, 0, 1, 0, 0, 0, 1)	6
	(0, 3, 1, 1, 0, 1, 0, 0)	6
	(0, 3, 0, 1, 0, 0, 1, 0)	18
$(0,4,1,1)_1$	(0, 2, 0, 0, 0, 0, 0, 2)	15
	(0, 3, 1, 0, 0, 1, 0, 1)	6
$(1,3,3,1)_0$	(1, 0, 0, 1, 0, 0, 3, 0)	2
	(1, 0, 0, 0, 0, 0, 3, 1)	3
(0, 6, 2, 0)	(0, 2, 0, 0, 0, 0, 0, 2)	6
	(0, 4, 1, 0, 0, 1, 1, 0)	3
	(0, 5, 1, 0, 0, 0, 1, 0)	12
(1, 5, 4, 0)	(1, 1, 1, 0, 0, 0, 2, 1)	3
(2, 4, 6, 0)	(0, 0, 1, 0, 0, 5, 1, 0)	3
	(0, 2, 1, 0, 0, 3, 1, 0)	3
	(0, 4, 2, 0, 0, 2, 0, 0)	6
	(1, 0, 1, 0, 0, 2, 3, 0)	3
	(1, 3, 3, 0, 0, 1, 1, 0)	3
(5, 3, 6, 0)	(4, 3, 4, 0, 0, 1, 0, 0)	3
	(5, 3, 6, 0, 0, 0, 0, 0)	1
(8, 2, 6, 0)	(5, 0, 2, 0, 2, 3, 0, 0)	3
	(4, 2, 4, 0, 3, 0, 0, 0)	3
(12, 0, 8, 0)	(6, 0, 0, 0, 7, 0, 0, 0)	3
(20, 0, 0, 0)	(20, 0, 0, 0, 0, 0, 0, 0)	1

Penrose tiles and the projected pattern of a decorated 6D hypercubic lattice is not clear, it is interesting that difficulty in obtaining a continuously connected network is a common feature.

5. Concluding remarks

In the continuous random network (CRN) model (Polk, 1971; Connell & Temkin, 1974) for amorphous semiconductors, aperiodicity is essentially achieved through the variation in the relative rotation angle of tetrahedral coordinations of adjacent atoms, θ. There a network is built by adding tetrahedral atoms one by one without leaving any dangling bond. Eventually, in the CRN model, the distribution of θ ($|\theta| \leq 60°$) comes out as a symmetric distribution peaked at $\theta = \pm 60°$ (Connell & Temkin, 1974; Polk & Boudreaux, 1973; Steinhardt, Alben & Wearie, 1974). In diamond, wurtzite and BC-8 structures, a network is a mixture of staggered ($\theta = \pm 60°$) and eclipsed ($\theta = 0°$) configurations with a bulk ratio 1:0, 3:1 and 1:3, respectively. In § 2 we investigated a system consisting of only eclipsed configuration. All these structures are continuously connected or, in other words, there are no broken bonds. In §§ 3 and 4 we examined systems involving icosahedral orientational order as well as tetrahedral bonding. In both cases broken bonds are necessarily introduced, although there still remains the possibility that broken bonds are saturated by bond rearrangement. In the polytope 240 model discussed in § 3, a template with definite chirality in a local atomic arrangement, which is associated with the sign of θ, is used to describe LPO. A defect associated with chirality is obviously a wall, on which tetrahedral bonds are generally broken. Although chirality is not clear in a decorated Penrose lattice, it is interesting that a periodic Penrose lattice decorated successfully with no broken bond is relaxed to a structure with a symmetric mixture of chirality. It would therefore be interesting to investigate a system without symmetry breaking in chirality.

The author acknowledges conversations with David Nelson, who suggested this problem. He also thanks all the members of the Condensed Matter Theory group at Harvard University for their hospitality. This work was supported by the National Science Foundation, through the Harvard Materials Research Laboratory and through Grant DMR 85-14638.

APPENDIX *A*

Quaternion representation of a 4D sphere

In this Appendix we summarize the description of the geometry of an S^3 manifold in terms of quaternion representations (Nelson & Widom, 1984).

The coordinates of a point of S^3 are parametrized by a geodesic distance ψ and coordinates on a three-dimensional unit sphere (x, y, z) as

$$(x_0, x_1, x_2, x_3) = (\cos\psi, x \sin\psi, y \sin\psi, z \sin\psi), \tag{A.1}$$

where $0 \leq \psi \leq \pi$. Here S^3 has a contact with a flat real space R^3 at its north pole $(1, 0, 0, 0)$. Usually it is more convenient to express the coordinates in terms of a quaternion as

$$\begin{aligned}\hat{u} &= \hat{1}\cos\psi + i\sin\psi(\hat{\sigma}_x x + \hat{\sigma}_y y + \hat{\sigma}_z z) \\ &= \exp[i\psi(\hat{\sigma}_x x + \hat{\sigma}_y y + \hat{\sigma}_z z)],\end{aligned} \tag{A.2}$$

where

$$\hat{\sigma}_\alpha \hat{1} = \hat{1}\hat{\sigma}_\alpha = \hat{\sigma}_\alpha, \tag{A.3}$$

$$\begin{aligned}\hat{\sigma}_\alpha\hat{\sigma}_\beta &= \hat{1}, && \alpha = \beta \\ &= i\varepsilon_{\alpha\beta\gamma}\hat{\sigma}_\gamma, && \alpha \neq \beta\end{aligned} \tag{A.4}$$

with an antisymmetric tensor $\varepsilon_{\alpha\beta\gamma}$. Since a rigid rotation in four dimensions is generated by six generators, a four-dimensional rotation is given in terms of left (l) and right (r) screw transformations as

$$\begin{aligned}(l, r):\ \hat{u} &= l\hat{u}r^{-1}, \\ &= \exp[i(\psi_l/2)(\hat{\sigma}\mathbf{n}_l)]\hat{u}\exp[-i(\psi_r/2)(\hat{\sigma}\mathbf{n}_r)],\end{aligned} \tag{A.5}$$

where

$$\hat{\sigma}\mathbf{n}_l = \hat{\sigma}_x n_{l_x} + \hat{\sigma}_y n_{l_y} + \hat{\sigma} n_{l_z}. \tag{A.6}$$

The generators of rotation in a flat space, L_{xy}, L_{yz} and L_{zx}, are expressed as

$$(l, l):\ \hat{u} = \exp[i(\psi_l/2)(\hat{\sigma}\mathbf{n}_l)]\hat{u}\exp[-i(\psi_l/2)(\hat{\sigma}\mathbf{n}_l)], \tag{A.7}$$

whereas the generators of rotation analogous to a flat-space translation, L_{0x}, L_{0y} and L_{0z}, are

$$(l, l^{-1}):\hat{u} = \exp[i(\psi_l/2)(\hat{\sigma}\mathbf{n}_l)]\hat{u}\exp[i(\psi_l/2)(\hat{\sigma}\mathbf{n}_l)]. \tag{A.8}$$

Here ψ_l is a rotational angle. Apparently rolling of S^3 along a straight line in R^3 induces a rotation of S^3 generated by (l, l^{-1}): (see Fig. 14).

A set of vertices of polytope $\{3, 3, 5\}$ is isomorphic to Y' where a vertex $(1, 0, 0, 0)$ corresponds to a unit element of Y' (see Appendix B). Let us consider a rolling along a straight line in R^3 which is a trace of a geodesic line between two vertices of polytope $\{3, 3, 5\}$, say $(1, 0, 0, 0)$ and $\exp[i\psi_0(\hat{\sigma}\mathbf{n}_0)]$. Then a vertex of the polytope, $\hat{u}$, is transformed by rolling as

$$\hat{u}' = (l, l^{-1}):\hat{u}, \tag{A.9}$$

where

$$l = \exp[i(\psi_0/2)(\hat{\sigma}\mathbf{n}_0)]. \tag{A.10}$$

Since l is not generally an element of Y', $\hat{u}'$ is not an element of Y'. In other words, the transformation associated with rolling is not a symmetry operation of the polytope. To clarify this meaning, let us rewrite (A.9) as

$$\hat{u}' = (l, l):[\hat{1}, (l^2)^{-1}]:\hat{u}. \tag{A.11}$$

Here, since l^2 is an element of Y', a set of transformed vertices $\{\hat{u}l^2\}$ agrees with a set of original vertices $\{\hat{u}\}$ (because of the so-called rearrangement theorem). Because the transformation (l, l): gives a rotation of an icosahedral arrangement around $\hat{u}l^2 = (1, 0, 0, 0)$, the rolling of polytope induces a rotation of a local atomic arrangement in a flat space R^3, which is not necessarily a symmetry operation of an icosahedron. Therefore the rolling polytope model automatically incorporates defects of orientational order, *i.e.* disclinations.

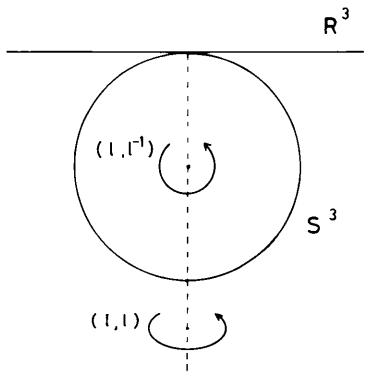

Fig. 14. Schematic illustration of rolling S^3.

Table 4. *Class multiplication table for the group T'*

	$\mathscr{C}_0$	$\bar{\mathscr{C}}_0$	$\mathscr{C}_3$	$\bar{\mathscr{C}}_3$	$\mathscr{C}_2$
$\mathscr{C}_0$	$\mathscr{C}_0$	$\bar{\mathscr{C}}_0$	$\mathscr{C}_3$	$\bar{\mathscr{C}}_3$	$\mathscr{C}_2$
$\bar{\mathscr{C}}_0$	$\bar{\mathscr{C}}_0$	$\mathscr{C}_0$	$\bar{\mathscr{C}}_3$	$\mathscr{C}_3$	$\bar{\mathscr{C}}_2$
$\mathscr{C}_3$	$\mathscr{C}_3$	$\bar{\mathscr{C}}_3$	$8\mathscr{C}_0+4\mathscr{C}_2+3\mathscr{C}_3+\bar{\mathscr{C}}_3$	$8\bar{\mathscr{C}}_0+4\bar{\mathscr{C}}_2+\mathscr{C}_3+3\bar{\mathscr{C}}_3$	$3\mathscr{C}_3+3\bar{\mathscr{C}}_3$
$\bar{\mathscr{C}}_3$	$\bar{\mathscr{C}}_3$	$\mathscr{C}_3$	$8\bar{\mathscr{C}}_0+4\bar{\mathscr{C}}_2+3\mathscr{C}_3+\bar{\mathscr{C}}_3$	$8\mathscr{C}_0+4\mathscr{C}_2+3\bar{\mathscr{C}}_3+\mathscr{C}_3$	$3\mathscr{C}_3+3\bar{\mathscr{C}}_3$
$\mathscr{C}_2$	$\mathscr{C}_2$	$\bar{\mathscr{C}}_2$	$3\mathscr{C}_3+3\bar{\mathscr{C}}_3$	$3\mathscr{C}_3+3\bar{\mathscr{C}}_3$	$6\mathscr{C}_0+6\bar{\mathscr{C}}_0+4\mathscr{C}_2$

APPENDIX *B*

Elements and classes of the groups *Y'* and *T'*

According to homotopy theory (Mermin, 1979), the class structure of the non-Abelian homotopy group determines how defects combine. The 120 elements of Y' are classified into nine classes as

$$\begin{aligned}
&\mathscr{C}_0 = \{1\},\\
&\mathscr{C}_5 = \{\exp[i(\pi/5)(\hat{\sigma}\mathbf{e}_v^{(j)})], j = 1, \ldots, 12\},\\
&\mathscr{C}_3 = \{\exp[i(\pi/3)(\hat{\sigma}\mathbf{e}_f^{(j)})], j = 1, \ldots, 20\},\\
&\mathscr{C}_5^2 = \{\exp[i(2\pi/5)(\hat{\sigma}\mathbf{e}_v^{(j)})], j = 1, \ldots, 12\},\\
&\mathscr{C}_2 = \{\exp[i(\pi/2)(\hat{\sigma}\mathbf{e}_e^{(j)})], j = 1, \ldots, 30\},\\
&\mathscr{C}_5 = \{\exp[i(3\pi/5)(\hat{\sigma}\mathbf{e}_v^{(j)})], j = 1, \ldots, 12\},\\
&\mathscr{C}_3 = \{\exp[i(2\pi/3)(\hat{\sigma}\mathbf{e}_f^{(j)})], j = 1, \ldots, 20\},\\
&\mathscr{C}_5 = \{\exp[i(4\pi/5)(7\sigma\mathbf{e}_v^{(j)})], j = 1, \ldots, 12\},\\
&\mathscr{C}_0 = \{-1\},
\end{aligned} \tag{B.1}$$

where $\mathbf{e}_v^{(j)}$, $\mathbf{e}_f^{(j)}$ and $\mathbf{e}_e^{(j)}$ denote unit vectors in the direction of fivefold, threefold and twofold symmetry axes of an icosahedron, respectively. The class multiplication table for Y' is given by Nelson (1983*a*). The 24 elements of T', which is a subgroup of Y', are classified into five classes as

$$\begin{aligned}
&\mathscr{C}_0 = \{1\},\\
&\mathscr{C}_3 = \{\exp[i(\pi/3)(\hat{\sigma}\mathbf{e}_3^{(j)})], j = 1, \ldots, 8\},\\
&\mathscr{C}_2 = \{\exp[i(\pi/2)(\hat{\sigma}\mathbf{e}_2^{(j)})], j = 1, \ldots, 6\},\\
&\mathscr{C}_3 = \{\exp[i(2\pi/3)(\hat{\sigma}\mathbf{e}_3^{(j)})], j = 1, \ldots, 8\},\\
&\mathscr{C}_0 = \{-1\},
\end{aligned} \tag{B.2}$$

where $\mathbf{e}_3^{(j)}$ and $\mathbf{e}_2^{(j)}$ are unit vectors in the direction of threefold and twofold symmetry axes of an tetrahedron, which are elements of subsets of $\{\mathbf{e}_f^{(j)}\}$ and $\{\mathbf{e}_e^{(j)}\}$, respectively. The class multiplication table for T' is given in Table 4.

APPENDIX *C*

Projection method generating Penrose lattice

A three-dimensional Penrose lattice is obtained by means of a projection of six-dimensional (6D) hypercubic lattice points onto a 3D real space. In this Appendix we will summarize the construction of a

3D Penrose lattice and its rational approximation by a projection method.

A complete set of six orthonormal vectors in 6D space is defined by

$$\left.\begin{aligned} |p_\parallel^{(1)}\rangle &= [2(\tau^2+1)]^{-1/2}(\tau, \tau, 1, 0, 0, 1), \\ |p_\parallel^{(2)}\rangle &= [2(\tau^2+1)]^{-1/2}(1, -1, 0, \tau, \tau, 0), \\ |p_\parallel^{(3)}\rangle &= [2(\tau^2+1)]^{-1/2}(0, 0, \tau, 1, -1, -\tau), \end{aligned}\right\} \quad (C.1)$$

$$\left.\begin{aligned} |p_\perp^{(1)}\rangle &= [2(\tau^2+1)]^{-1/2}(1, 1, -\tau, 0, 0, -\tau), \\ |p_\perp^{(2)}\rangle &= [2(\tau^2+1)]^{-1/2}(-\tau, \tau, 0, 1, 1, 0), \\ |p_\perp^{(3)}\rangle &= [2(\tau^2+1)]^{-1/2}(0, 0, 1, -\tau, \tau, -1), \end{aligned}\right\} \quad (C.2)$$

where τ is the golden mean. The projection operator onto a 3D physical space is given by

$$\hat{P}_\parallel = \sum_{j=1}^{3} |p_\parallel^{(j)}\rangle\langle p_\parallel^{(j)}|, \quad (C.3)$$

and that onto a 3D perpendicular space is given by

$$\hat{P}_\perp = \sum_{j=1}^{3} |p_\perp^{(j)}\rangle\langle p_\perp^{(j)}|. \quad (C.4)$$

Here a set of three vectors in a 3D physical space, $\{|p_\parallel^{(j)}\rangle\}$, is chosen so that a projection of six lattice vectors of a 6D hypercubic lattice gives six vertex vectors of an icosahedron. A 6D hypercubic lattice point is accepted to be projected onto a 3D physical space if its image in a 3D perpendicular space is in a compact shadow space $\mathcal{S}$. Then the lattice points of a 3D Penrose lattice are obtained as

$$\mathbf{R} = (\langle p_\parallel^{(1)}|n\rangle, \langle p_\parallel^{(2)}|n\rangle, \langle p_\parallel^{(3)}|n\rangle), \quad (C.5)$$

where a 6D hypercubic lattice point $|n\rangle = (n_1, n_2, n_3, n_4, n_5, n_6)$ (n_i's are integers) is accepted if the condition

$$\hat{P}_\perp|n\rangle \in \mathcal{S} \quad (C.6)$$

is satisfied. The shadow space $\mathcal{S}$ is typically chosen as an image of a 6D hypercubic unit cell.

When we replace τ in (C.2) by its rational approximation F_{k+1}/F_k where F_k is a Fibonacci number defined by $F_{k+1} = F_k + F_{k-1}$ with $F_0 = 0$ and $F_1 = 1$, we get a large cubic unit-cell structure (Elser & Henley, 1985) because there exists a non-trivial set of integers, $|\nu\rangle = (\nu_1, \nu_2, \nu_3, \nu_4, \nu_5, \nu_6)$, which satisfies

$$\hat{p}_\perp^{(\text{approx})}|\nu\rangle = (0, 0, 0, 0, 0, 0). \quad (C.7)$$

Elser & Henley (1985) referred to this system as an F_{k+1}/F_k structure. Here four F_{3k+2} prolate and four F_{3k+1} oblate rhombohedra are in a cubic unit cell whose size is given by $[2(\tau F_{k+1} + F_k)/(\tau^2+1)^{1/2}]^3$ where the edge length of Penrose rhombohedral tiles is taken to be unity.

References

BISWAS, R. & HAMMAN, D. R. (1985). *Phys. Rev. Lett.* **55**, 2001-2004.

CARGILL, G. S. III (1975). *Solid State Physics*, Vol. 30, edited by H. EHRENREICH, F. SEITZ & D. TURNBULL, pp. 227-320. New York: Academic Press.

COLLINS, R. (1972). *Phase Transition and Critical Phenomena*, Vol. II, edited by C. DOMB & M. S. GREEN, pp. 271-303. New York: Academic Press.

CONNELL, G. A. N. & TEMKIN, R. J. (1974). *Phys. Rev. B*, **9**, 5323-5326.

COXETER, H. S. M. (1983). *Regular Polytopes*. New York: Dover.

CROS, C., POUCHARD, M. & HAGENMULLER, P. (1970). *J. Solid State Chem.* **2**, 570-581.

ELSER, V. & HENLEY, C. L. (1985). *Phys. Rev. Lett.* **55**, 2883-2886.

FINNEY, J. L. (1970). *Proc. R. Soc. London Ser. A*, **319**, 479-493.

FRANK, F. C. (1952). *Proc. R. Soc. London Ser. A*, **215**, 43-46.

FRANK, F. C. & KASPER, J. S. (1958). *Acta Cryst.* **11**, 184-190.

FRANK, F. C. & KASPER, J. S. (1959). *Acta Cryst.* **12**, 483-499.

HENLEY, C. L. (1986). *Phys. Rev. B*, **34**, 797-816.

HENLEY, C. L. (1987). *Comments Condens. Matter Phys.* **13**, 59-118.

HENLEY, C. L. & ELSER, V. (1986). *Philos. Mag.* B**53**, L59-L66.

KASPER, J. S. & RICHARDS, S. M. (1964). *Acta Cryst.* **17**, 752-755.

KEATING, P. N. (1966). *Phys. Rev.* **145**, 637-645.

KLÉMAN, M. & SADOC, J. F. (1979). *J. Phys. (Paris) Lett.* **40**, L569-L574.

LEVINE, D. & STEINHARDT, P. J. (1984). *Phys. Rev. Lett.* **53**, 2477-2480.

MACKAY, A. L. (1985). *Nature (London)*, **315**, 636-636.

MERMIN, N. D. (1979). *Rev. Mod. Phys.* **51**, 591-648.

MOSSERI, R., DIVICENZO, D. P., SADOC, J. F. & BRODSKY, M. (1985). *Phys. Rev. B*, **32**, 3974-4000.

NELSON, D. R. (1983*a*). *Phys. Rev. B*, **28**, 5515-5535.

NELSON, D. R. (1983*b*). *Phase Transition and Critical Phenomena*, Vol. VII, edited by C. DOMB & J. L. LEBROWITZ, pp. 1-99. New York: Academic Press.

NELSON, D. R. & HALPERIN, B. I. (1979). *Phys. Rev. B*, **19**, 2457-2484.

NELSON, D. R. & WIDOM, M. (1984). *Nucl. Phys. B*, **240** (FS12), 113-139.

OLAMI, Z. & ALEXANDER, S. (1987). Preprint.

PAULING, L. (1960). *The Nature of the Chemical Bond*, ch. 4. Ithaca: Cornell Univ. Press.

POLK, D. E. (1971). *J. Non-Cryst. Solids*, **5**, 365-376.

POLK, D. E. & BOUDREAUX, D. S. (1973). *Phys. Rev. Lett.* **31**, 92-95.

RUBINSTEIN, M. & NELSON, D. R. (1983). *Phys. Rev. B*, **28**, 6377-6386.

SACHDEV, S. & NELSON, D. R. (1985). *Phys. Rev. B*, **32**, 1480-1502.

SADOC, J. F. & MOSSERI, R. (1982). *Philos. Mag.* **45**, 467-483.

SETHNA, J. P. (1985). *Phys. Rev. B*, **31**, 6278-6297.

SHECTMAN, D., BLECH, I., GRATIAS, D. & CAHN, J. W. (1984). *Phys. Rev. Lett.* **53**, 1951-1953.

SHENKER, J. L. *et al.* (1981). *Nature (London)*, **294**, 340-342.

STEINHARDT, P., ALBEN, R. & WEARIE, D. (1974). *J. Non-Cryst. Solids*, **15**, 199-214.

STEINHARDT, P. J., NELSON, D. R. & RONCHETTI, M. (1983). *Phys. Rev. B*, **28**, 784-805.

WELLS, A. F. (1977). *Three-Dimensional Nets and Polyhedra*, ch. 9. New York: John Wiley.

WIDOM, M. (1987). *Nonlinearity in Condensed Matter*, pp. 330-337. Berlin: Springer.

ZHANG, Q. M., KIM, H. K. & CHAN, M. H. W. (1985). *Phys. Rev. B*, **32**, 1820-1823.